Subm to "Photosensitivity and Quadratic Nonlinearity in Glass Waveguides: Fundamentals and Applications" '95

LASER INDUCED PRESSURE PULSE PROBE OF CHARGE DISTRIBUTION IN THERMALLY POLED GLASS: EVIDENCE OF DIPOLE POLARIZATION?

1058

P.G. Kazansky, A.R. Smith and P.St.J. Russell

Optoelectronics Research Centre, University of Southampton,
Southampton SO17 2BJ, United Kingdom

G. M. Yang and G. M. Sessler
Institute for Electroacoustics, Technical University of Darmstadt,
Darmstadt D-64293, Germany

Abstract

For the first time charge distributions in thermally poled silica glass are mapped by using laser induced pressure pulse technique. The experimental results may be explained through postulating the formation of both real space charge layers and *dipole polarization* inside the the depletion region.

LASER INDUCED PRESSURE PULSE PROBE OF CHARGE DISTRIBUTION IN THERMALLY POLED GLASS: EVIDENCE OF DIPOLE POLARIZATION?

P.G. Kazansky, A.R. Smith and P.St.J. Russell

Optoelectronics Research Centre, University of Southampton,
Southampton SO17 2BJ, United Kingdom

G. M. Yang and G. M. Sessler
Institute for Electroacoustics, Technical University of Darmstadt,
Darmstadt D-64293, Germany

In recent years, thermal poling of silica-based glasses has been shown to create permanent second-order nonlinearities (SON) of the order of 1 pm/V in bulk glass [1] and 0.2 pm/V in thermally poled optical fibre [2]. Despite the reproducibility and stability of the effect, the underlying mechanism has still not been fully elucidated.

In thermal poling of fused silica, samples 1-3 mm thick are heated to about 280°C with an applied voltage of about 5 kV, the second-order nonlinearity being observed near the anodic surface [1] and in the whole volume of the glass sample [3]. It has been suggested that a high electrostatic field, appearing in a thin depletion region near the anodic surface, is responsible for the anodic poling phenomenon. Indeed, under the action of the applied field, cations (such as Na^+ and H^+) will drift to the cathode leaving behind a *negatively* charged layer near the anodic surface. A high electrostatic field will then appear in this layer, peaking at the interface between the *negatively* charged layer and the anode.

In one scenario, this field creates a permanent $\chi^{(2)}$ by orientation of dipoles (or bonds) [4]. In another scenario [5], the very high field at the glass/anode boundary causes ionization of the glass (or perhaps the air gap), leading to the creation of a *positively* charged layer at the anodic surface. A high field then appears between this layer and the remaining *negatively* charged depletion layer deeper in the glass.

Experimental support for the second mechanism was obtained by testing the ratio of nonlinear tensor components and the spatial distribution of the induced $\chi^{(2)}$. These do not, however, disprove the dipole polarization mechanism [5]. Therefore, other experiments which yield further information about the charge distribution inside the glass are necessary for clarification of the mechanism. An example is the Laser Induced Pressure Pulse (LIPP) method, which is widely used for characterisation of the charge distribution in electrets [6,7]. In this paper we report for the first time the use of this method to map the charge profiles in thermally poled silica glass samples.

Fused silica glass samples were poled at 280°C at 5 kV applied voltage in an air atmosphere. During poling, the thinner samples I, II and III (~ 100 μm thick) were placed on top of a ~ 3 mm thick supporting substrate of Herasil 1 (this avoided electrical breakdown of the sample). They were then poled for 45 min, 15 min and 5 min respectively. Samples IV and V (~ 1 mm thick) were poled for 15 min. Samples I, II, III and IV were poled via a pressed-on electrode, and sample V was poled via a sputtered aluminium anodic electrode about 300 nm thick. Similar aluminium electrodes were sputtered (*after* poling) on to the cathode side

of each of the samples I, II, III and IV. Sputtered aluminium electrodes were used as front electrodes in all our LIPP studies (Fig.1).

In the LIPP measurements, single laser pulses of about 70 ps duration and 50 mJ energy, generated by a Nd:YAG laser, were used. These pulses were incident on an absorbing layer coated on to the front electrode of the samples. This excites acoustic pulses of <500 ps duration in the samples (Fig.1). The resulting pressure pulse causes any free charge to move, giving rise to an electrical current proportional to the sum of space-charge density and dipole-polarization gradient. The time axis can be transformed into a depth scale via the longitudinal sound velocity, which is approximately 5.95 km/s in fused silica (Fig.2). With these pulses, the spatial resolution of the LIPP technique turns out to be of about 3 μm. No LIPP signal was observed near the cathodic side of the samples. The cathodic side in sample I corresponds to positions 1, 3 and 5 of the pressure pulse (Fig.2a).

The first group of LIPP signals is generated after a single pass of the pressure pulse along the sample. The second group of signals is generated by the pressure pulse after one reflection from the rear (anodic) surface and one reflection from the front (cathodic) surface of the sample. And the third group of signals is generated by the pressure pulse after two reflections from the rear (anodic) surface and two reflections from the front (cathodic) surface of the sample. The positive signal spikes in positions 2, 4 and 5 correspond to a positive charge on the anodic surface and the two symmetrical spikes on both sides of the positive spike correspond to a negative charge at a depth of about 5.5 μm below the anodic surface. The first negative spike is caused by the incident acoustic pulse and the closely spaced second negative spike by the reflected pulse. The measured ratio of LIPP signals in samples I, II and III poled for different times is about 9:3:1.

We were surprised to observe that the LIPP scans of the samples IV and V revealed completely the opposite charge distribution (Fig.2b and Fig.2c). Notice that only the single pass LIPP signals are measured in these thick samples and that the front electrode is located at the anodic surface of sample V. Under these conditions a negative LIPP spike corresponds to a negative charge at the anodic surface, the two symmetric positive spikes (caused by incident and reflected pressure pulses) to a positive charge at a depth of about 10 μm below the anodic surface, and the two small symmetric negative LIPP signals to a small negative charge at a depth of about 20 μm below the anodic surface of sample IV (Fig.2b). In sample V the first LIPP spike (positive) corresponds to a positive charge at the front electrode, the second spike (negative) to a negative charge at a depth of about 5 μm below the anodic surface, the third spike (positive) to a positive charge at a depth of about 10 μm and finally the fourth spike (negative) to a negative charge at a depth of about 30 μm below the anodic surface (Fig.2c).

These measurements were carried out 5 days after poling. Repeating them on samples I, II and III 26 days after poling, the LIPP signals were reduced and the charge distribution had changed to look similar to that first observed in sample IV (Fig.2d). However, no significant change in the LIPP signals was observed after repeated measurements in samples IV and V. Notice that the LIPP signal is inversely proportional to the gap between the electrodes (sample thickness). Therefore the initial normalised LIPP signals, and their corresponding charge densities in thin samples I, II and III, were about 3, 9 and 27 times smaller than in samples IV and V, which showed a stable charge distribution.

These experimental results may be interpreted as follows. A positive layer at the surface of the samples (caused either by high field ionization in the sample or by attraction of positively charged ions from the air) and a negatively charged layer deeper in the samples (caused by depletion of cations) are the "real" space charge layers. However, the reversed charge distributions are difficult to explain using "real" space charge. The most logical interpretation of these anomalous distributions is as bound charge caused by the gradient of the dipole polarization at the edges of the depletion region. It is possible to explain the observed transformation of the charge distributions in the thin samples by low stability of the poled layer in these not sufficiently poled samples where the space charge field is not compensated by the field of the bound charges. Indeed, in these samples the space charge field is initally higher than the electric field caused by dipole polarization, but it decays with time, revealing the dipole polarisation.

In conclusion, the charge distribution in thermally poled glass can be successfully characterised by the LIPP technique. The experimental results may be explained through postulating the formation of both real space charge layers and *dipole polarization* inside the the depletion region.

References

1. R. A. Myers, N. Mukherjee, and S. R. J. Brueck, Opt. Lett. **16**, 1732 (1991).
2. P. G. Kazansky, L. Dong, and P. St. J. Russell, Opt. Lett. **19**, 701 (1994).
3. H. Nasu, H. Okamoto, A. Mito, J. Matsuoka, and K. Kamiya, Jpn. J. Appl. Phys. **32**, L406 (1993).
4. N. Mukherjee, R. A. Myers, and S. R. J. Brueck, J. Opt. Soc. Am. **B**, 665 (1994).
5. P.G. Kazansky and P. St. J. Russell, Opt. Comm. **110**, 611 (1994).
6. G. M. Sessler, J. E. West, and G. Gerhard, Phys. Rev. Lett. **48**, 563 (1982).
7. G. M. Yang, S. Bauer-Gogonea, G. M. Sessler, S. Bauer, R. Ren, W. Wirges, and R. Gerhard-Multhaupt, Appl. Phys. Lett. **64**, 22 (1994).

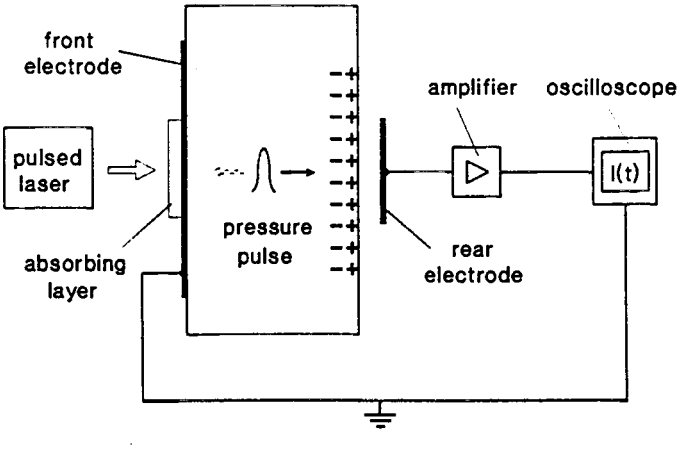

Fig.1 Experimental setup for the LIPP method

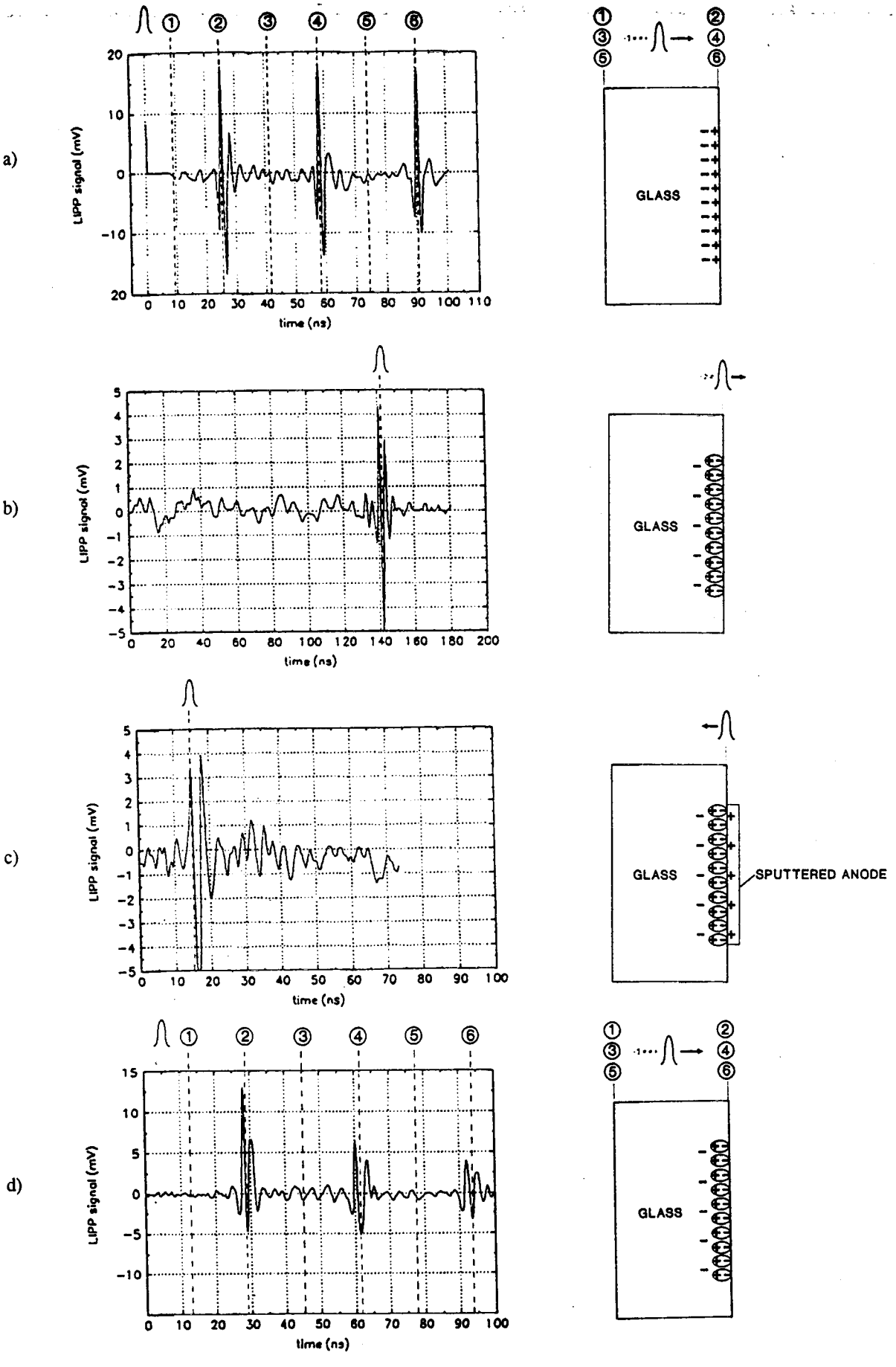

Fig.2 LIPP scans and corresponding charge profiles 5 days after poling in samples I (a), IV (b), V (c) and 26 days after poling in sample I (d).